

# A Solar PV Model Parameter Estimation Based on the Enhanced Self-Organization Maps

Mouncef El Marghichi<sup>1\*</sup>

<sup>1</sup> Faculty of Sciences and Technology, Hassan first University, 26002 Settat, P.O.B. 577, Morocco

\* Corresponding author, e-mail: [m.elmarghichi@uhp.ac.ma](mailto:m.elmarghichi@uhp.ac.ma)

Received: 15 March 2023, Accepted: 21 June 2023, Published online: 07 August 2023

## Abstract

Solar photovoltaic (PV) is a commonly utilized renewable energy source, with PV cells often being modeled as electric circuits. The identification of suitable circuit model parameters for PV cells is vital for performance evaluation, efficiency calculations, and the implementation of maximum power point tracking in solar PV systems. However, modeling the solar PV system is a nonlinear problem that requires an efficient algorithm. In this paper, we employ the enhanced self-organization maps (EASOM) to efficiently reduce the search space for parameter estimation in solar PV models. Our algorithm trains the SOM network on a subset of solutions, identifies the top solution's neural unit, generates a population of potential solutions, and selects the best candidate using a cost function, which represents the best PV model parameters obtained. The performance of EASOM is verified by extracting the parameters of the single diode (SDM) and double diode (DDM) models for the STM6-40/36 PV module. EASOM outperformed state-of-the-art algorithms with the lowest RMSE and MSE values of 8.3 mA and 6.87e-05 and achieved the lowest maximum error values of 27.37 mA and 20.52 mA, as well as low power error of 66.04 mW and 62.8 mW for SDM and DDM models.

## Keywords

enhanced self-organization maps (EASOM), PV parameter extraction, PV model, solar PV

## 1 Introduction

The use of renewable energy sources has been on the rise due to various factors related to climate change and energy crises. Solar power systems are commonly used in large-scale photovoltaic power plants to generate electricity especially in strong sunlight countries [1, 2]. However, these systems are often installed in exposed areas and can be vulnerable to deteriorating conditions during severe weather, such as rainstorms and gales. To address this issue, precise data-driven models are needed to determine the fundamental properties of photovoltaic systems in the solar industry. Analyzing the parameters of solar models is advantageous for evaluating the performance of photovoltaic power plants, calculating efficiency, implementing maximum power point tracking (MPPT), and optimizing energy management of the system [3].

Detailed modeling of solar photovoltaic systems involves two stages: mathematical model development and parameter identification. The single-diode model (SDM) and double-diode model (DDM) are widely used in all models [4]. However, the actual performance of

these models can be affected by unspecified parameters, which may cause them to become unstable and prone to errors when subjected to equipment aging or other contingencies. Therefore, accurately estimating the parameters of photovoltaic cell models is crucial [5]. Furthermore, the installation and optimization of photovoltaic systems should be done with more precision. However, the photovoltaic model is a nonlinear system with a non-convex relationship, which poses several challenges and obstacles. To address these issues, researchers have made significant efforts to identify methods for accurately estimating unknown parameters. Three broad approaches have been identified: analytical methods, deterministic methods, and metaheuristic methods [6].

Analytical methods for estimating parameters involve analyzing data provided by the supplier, including open-circuit voltage, short-circuit current, maximum power point, and I-V characteristics. These methods use all data points on the I-V characteristic curve to determine the parameters that minimize the difference between predicted and

measured values [7]. Although analytical methods are simple, fast, and unique, they rely on various mathematical formulas that are often simplified based on assumptions. These assumptions can lead to less accurate parameter estimates because some of the formulas may not hold true in practice.

Deterministic methods estimate unknown parameters by using a "take all measured data for the entire system" approach. These methods require a significant number of measurements to accurately extract the parameters [8, 9]. They are based on an objective function that measures the difference between the measured and predicted data points. However, because deterministic methods use gradient information, they may only converge towards a local optimal solution.

In contrast, evolutionary-based algorithms, such as the genetic algorithm (GA) [10], differential evolutionary algorithm (DEA) [11], and evolutionary strategy algorithm (ESA) [12], are developed based on the principles of evolution. These algorithms are designed to search for the optimal solution in a large parameter space and can provide more accurate estimates than deterministic methods.

Metaheuristic methods are similar to deterministic methods in that they also use the "take all real measured data for the whole system" approach. However, metaheuristic methods are considered some of the best global optimization algorithms due to their robustness, reliability, simplicity, and ease of implementation. These methods use biological processes to find optimal solutions for real-world problems and have gained attention in recent years.

Metaheuristic algorithms can be grouped into different categories, such as evolutionary-based algorithms (e.g., genetic algorithm, differential evolutionary algorithm), swarm-based algorithms (e.g., particle swarm optimization [13], ant colony optimization [14]), physics-based algorithms (e.g., gravitational search algorithm [15]), and human behavior-based algorithms (e.g., teaching-learning based optimization [16], political optimizer [17]). For a summary of the most common techniques used to extract PV solar model parameters, please refer to Table 1.

To model PV cells and modules accurately, analog electrical circuits are often used. Photovoltaic researchers typically prefer using DDM and SDM modeling techniques. For single-diode cells and modules, five parameters are required for simulation, while double-diode cells and modules require seven parameters. To achieve accurate simulation of the I-V characteristics of the physical system, it is essential to estimate the PV cell/module's parameters precisely, with minimal absolute error between the predicted and measured PV cell/module currents.

**Table 1** Summary of the common method used to extract the solar PV cell parameters

Approach	Advantages	Disadvantages
Analytical methods	Simplicity, speed, and uniqueness	Derived parameters may not be accurate, assumptions based
Deterministic methods	Objective function for difference between experimental and estimated data, converges to local best optimum solution	Requires a relatively large number of measurements, based on gradient information
Metaheuristic methods	Global best optimization algorithms, robustness, performance reliability, simplicity, ease of implementation	May require more computational resources, not guaranteed to find the optimal solution, tuning parameters may be difficult

Previous research has identified gaps in metaheuristic optimization and solar cell parameter identification. These gaps include non-adaptive weight parameters in metaheuristic algorithms, the potential for metaheuristic algorithms to become trapped in local best optima, and the need to further minimize the RMSE (root mean square error) values obtained by most algorithms.

To address the shortcomings of solar cell parameter extraction, we propose a novel metaheuristic algorithm called "Enhanced Self-Organization Maps", which utilizes self-organization maps (SOM) to minimize the search space required for parameter estimation in solar PV models. Our approach involves training the SOM network on a specific set of solutions, determining the neural unit that corresponds to the top solution, generating a pool of potential solutions, and ultimately selecting the most suitable candidate (the optimal solar PV parameter) based on a cost function.

The proposed algorithm is highly efficient, capable of achieving the global best optimum value with fewer iterations. It has been tested and shown to be robust and efficient, making it a suitable method for estimating parameters in solar PV models.

The paper makes the following main contributions:

- Novel approach: this paper introduces a novel approach to address the gaps that exist in metaheuristic optimization and solar cell parameter identification. The proposed approach offers innovative solutions to enhance the accuracy and reliability of parameter estimation in these areas.
- Robustness and effectiveness: the algorithm proposed in this paper has been extensively tested and demonstrated to be robust and effective in accurately

estimating parameters for both single-diode (SDM) and double-diode (DDM) models of solar cells. The algorithm showcases its capability to handle various complexities and provide reliable results.

- Comparative evaluation: the paper provides a comprehensive comparison of the proposed algorithm against four well-known and robust algorithms in the field: SFO (Sunflower Optimization Algorithm), WOS (War Strategy Optimization Algorithm), modified JAYA, and GBO (Gradient-Based Optimizer). This comparative analysis highlights the strengths and advantages of the proposed algorithm over these existing approaches.

### 1.1 Benefits and drawbacks of the proposed algorithm

The proposed EASOM presents several strengths and limitations. One of its main strengths is its ability to accurately estimate the parameters of solar PV models with minimal absolute error between the predicted and measured PV cell/module currents. Additionally, the use of self-organization maps (SOM) helps to minimize the search space required for parameter estimation, making it a highly efficient method capable of achieving the global best optimum value with fewer iterations. Furthermore, the algorithm has been shown to be robust and effective in estimating the parameters of both single-diode and double-diode solar PV models. However, there are also limitations to the EASOM algorithm. One such limitation is its slow run time, which could be improved in future iterations of the algorithm. Another limitation is its reliance on a cost function to select the most suitable candidate, which may not always accurately reflect the desired outcome. Additionally, while the algorithm has been tested and shown to be effective, further validation and testing may be necessary to ensure its accuracy and reliability in a variety of applications.

### 1.2 Paper organization

The document is organized as follows: in Section 2, we present the solar PV models used in this research, along with the required equations. Section 3 outlines the steps involved in implementing the algorithm, including the implementation setup for the STM6 test. In Section 4, we present and discuss in detail the results of the algorithm. Section 5 describes the applications of the present work, recommendations, and future scope to other researchers, and Section 6 concludes the paper with final remarks.

## 2 SOLAR PV modeling

The focus of Section 2 is on the mathematical models used for solar PV cells and modules.

### 2.1 Single-Diode Model (SDM)

The I-V characteristics of PV modules can be represented by various equivalent circuits, the SDM is the most widely used model due to its simplicity and high accuracy [16, 18]. This mathematical model uses a single-diode approximation to establish the relationship between different variables [19]. As shown in Fig. 1, the SDM consists of several parameters, including  $I$  (output current),  $I_{sh}$  (shunt resistance current),  $R_s$  (series resistance),  $I_{ph}$  (photocurrent),  $I_D$  (diode current), and  $R_{sh}$  (shunt resistance) [20].

Equations (1) and (2) provide mathematical expressions for  $I_D$  and  $I_{sh}$ , respectively:

$$I_D = I_{sd} \left( \exp \left( \frac{q(V + IR_s)}{nKT} \right) - 1 \right), \quad (1)$$

$$I_{sh} = \frac{V + IR_s}{R_{sh}}, \quad (2)$$

with:

$$I = I_{ph} - I_{sh} - I_D, \quad (3)$$

The output current is outlined by Eq. (4):

$$I = I_{ph} - I_{sd} \left( \exp \left( \frac{q(V + IR_s)}{nKT} \right) - 1 \right) - \frac{V + IR_s}{R_{sh}}. \quad (4)$$

The  $I_{sd}$  represents the reverse diode saturation current.  $q$  refers to the electron charge (1.602e-19 C),  $K$  represents the Boltzmann constant, the cell output voltage is depicted by  $V$ ,  $R_s$  is the series resistance,  $n$  is the diode ideality factor,  $T$  is the temperature in kelvin, and  $R_{sh}$  is the shunt resistance [21].

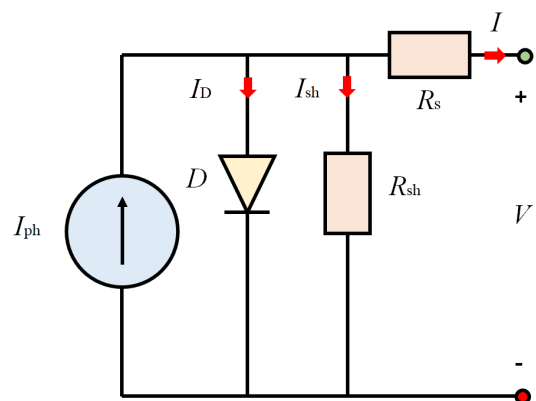


Fig. 1 SDM equivalent circuit

### 2.2 Double-Diode Model (DDM)

The Double-Diode Model (DDM) is another circuit model used to address the energy loss issue not considered by the SDM. Fig. 2 shows the DDM circuit. The current  $I$  flowing in the DDM circuit is calculated as follows (Eq. (5)):

$$I = I_{ph} - I_{D1} - I_{D2} - I_{sh}. \quad (5)$$

The symbols  $I_{D2}$  and  $I_{D1}$  represent the currents flowing through the second and first diodes, respectively.

$$I_{D1} = I_{sd1} \left( \exp\left(\frac{q(V + IR_s)}{n_1KT}\right) - 1 \right) \quad (6)$$

$$I_{D2} = I_{sd2} \left( \exp\left(\frac{q(V + IR_s)}{n_2KT}\right) - 1 \right) \quad (7)$$

In Eqs. (6) and (7)  $I_{sd1}$  and  $I_{sd2}$  are the reverse diode saturation currents of the diodes. The current  $I$  can be calculated using Eq. (8) where  $n_2$  and  $n_1$  represent the ideality factor of the diodes:

$$I = I_{ph} - I_{sd1} \left( \exp\left(\frac{q(V + IR_s)}{n_1KT}\right) - 1 \right) - I_{sd2} \left( \exp\left(\frac{q(V + IR_s)}{n_2KT}\right) - 1 \right) - \frac{V + IR_s}{R_{sh}}. \quad (8)$$

### 2.3 PV module model

The output current ( $I$ ) of a photovoltaic (PV) module, composed of  $N_p \times N_s$  solar cells arranged in parallel and/or series, can be calculated using Eq. (9).

In the case of using the SDM-based PV module:

$$I = I_{ph} - I_{sd} \left( \exp\left(\frac{q \left( \frac{V}{N_s} + \frac{IR_s}{N_p} \right)}{nKT}\right) - 1 \right) - \frac{IR_s / N_p + V / N_s}{R_{sh}}. \quad (9)$$

For the DDM:

$$I = I_{ph} - I_{sd1} \left( \exp\left(\frac{q \left( IR_s / N_p + V / N_s \right)}{n_1KT}\right) - 1 \right) - I_{sd2} \left( \exp\left(\frac{q \left( V / N_s + IR_s / N_p \right)}{n_2KT}\right) - 1 \right) - \frac{IR_s / N_p + V / N_s}{R_{sh}}. \quad (10)$$

### 2.4 Objective function

The primary objective is to minimize the difference between the simulated and measured current while estimating the parameters of the solar cell. The RMSE (root mean square error) is a commonly used and accurate method to achieve this goal by serving as an objective

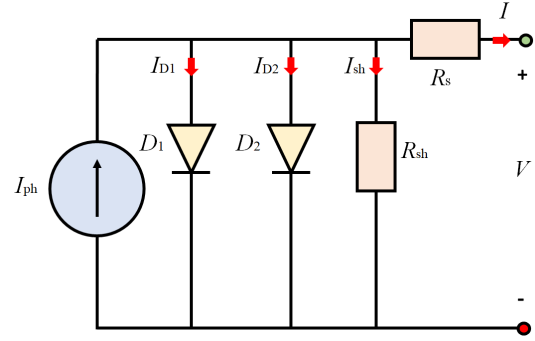


Fig. 2 DDM equivalent circuit

function to determine the best parameter values for the PV model. In this study, we use the EASOM algorithm to extract the parameters of a solar PV system by measuring its current and voltage. The cost function is created based on the discrepancy between the predicted and measured current values, which is measured by:

$$F_{loss} = \sqrt{\frac{1}{N} \left( \sum_{i=1}^N |I_{estim} - I_{mes}|^2 \right)}. \quad (11)$$

In Eq. (11)  $I_{estim}$  and  $I_{mes}$  are respectively the estimated and measured output current.

### 3 EASOM algorithm

The EASOM algorithm, introduced in [22], is designed to solve nonlinear optimization problems with bounded constraints. The algorithm can be formulated as follows (Eq. (12)):

$$\text{maximize } f(x), \quad x = w_j (x^1, x^2 \dots x^n) \in \mathbb{R}, \quad (12)$$

where the subject:  $x \in X$ .

The proposed algorithm aims to solve nonlinear optimization problems within a specific search space  $X$  that is bounded by lower and upper bounds. The function  $f(x)$  represents the nonlinear mapping. The algorithm starts at an initial point ( $k = 0$ ) and proceeds to a maximum iteration limit ( $k = Maxgen$ ). First, a set of candidate solutions is generated, which is four times the number of solutions generated in each subsequent iteration ( $k \neq 0$ ). Then, a self-organizing map (SOM) is trained on this initial set in the first stage to identify promising areas and reduce the search space. In each iteration, a subset of previously generated solutions is used to train the SOM. After training, the neuronal unit in the lattice that corresponds to the optimal solution is identified. Using this information, a complete set of potential solutions is generated. The algorithm can be summarized in six steps (Sections 3.1 to 3.6).

### 3.1 Initialization

To initiate the EASOM algorithm, a set of  $(2N)$  potential solutions, denoted as  $P(k)$ , is randomly generated within the boundaries  $(li)$  and  $(ui)$ . Each item in  $P(k)$ , represented as  $pi(k)$ , is an  $n$ -sized element that proposes a potential solution for the optimization problem. During the evolutionary process, a fitness value is assigned to each  $pi(k)$  based on the loss function  $f(pi(k))$ . The best solution discovered so far,  $g (g_1, g_2, \dots, g_n)$ , is recorded as the optimal solution during the optimization process. Additionally, all components of  $P(k)$  are stored in a memory  $H(k)$ , which contains all generated solutions.

### 3.2 Training

The EASOM algorithm utilizes a self-organizing map to reduce the search space and identify potential regions. The SOM (as shown in Fig. 3) has an input layer with  $n$  nodes and a lattice size of  $n$  by  $n$ . The algorithm uses a set of  $(2N)$  data points, denoted as  $T(k)$ , to train the SOM. The parameters  $d_0$  and  $a_0$  are set to 10 and 1, respectively, and the SOM is trained for 100 epochs. During the learning process, each input data point is a tuple  $ti = \{pi(k), f(pi(k))\}$ , which combines a potential solution with its corresponding fitness value. Initially,  $T(0)$  is set to the first population, and in each iteration, the algorithm updates  $T(k)$ . The quality of the space search reduction is determined by the number of samples used in the training process, with a larger sample size leading to better outcomes at the cost of increased computational requirements.

### 3.3 Data retrieval (extraction)

The SOM algorithm is designed to preserve the topological structure of input data, allowing similar data units to be represented by adjacent neurons on the output lattice. This property makes it easier to visualize complex data structures. In the context of the EASOM algorithm, the SOM is

trained with the set of potential solutions generated by the algorithm to extract useful information about the search space. After training, the SOM is used to identify regions of the search space that correspond to the best solutions found so far. This is done by locating the neural unit  $W_w$  on the competitive lattice layer that best matches the current best solution  $g$ . The selected neural unit  $w$  has weights that are closest to  $g$ , satisfying the following condition:

$$w = \min \{W_w - g\}. \tag{13}$$

To extract information from the competitive layer, the EASOM algorithm retrieves the local knowledge surrounding the neuronal unit  $W_w$ . This is done by identifying the two neighboring units,  $W_A$  and  $W_B$ , with weights closest to the optimal solution  $g$ , regardless of the presence of the  $W_w$  unit. The distances between each of these units and  $g$  are also recorded. These distances are calculated using the following formula:

$$D_w = W_w - g, D_B = W_B - g, D_A = W_A - g. \tag{14}$$

After identifying the optimal solution  $g$  through its corresponding neural unit  $w$ , the location of this unit in the  $n \times n$  lattice serves as a reference point for spatial mapping. The objective is to establish a connection between the original location of the data and its mapped location in the lattice. To achieve this, a positional rank  $R$  is calculated, which reflects the relative position of the mapped data unit with respect to the optimal solution unit in the lattice. The positional rank  $R$  is computed in Eq. (15):

$$R = 1 - \frac{|m - w|}{n}. \tag{15}$$

The value of  $R$  rank is determined by the position of the lattice core unit, which is located at  $m = n \times n / 2$ . The  $R$  rank has a value close to one at the center of the lattice and decreases towards zero as it approaches the edge.

### 3.4 Production of the solution

Under the EASOM framework, the information gathered during the algorithm's operation is utilized to guide its search strategy. After identifying potential areas and locating them in the neural lattice, a pool of  $N$  new solutions is generated. In the SOM, the input data units are assigned to a single neural layer in the competitive layer. In this case, the new set of solutions is generated assuming that their locations are highly likely to be within a radius of influence surrounding the successful neural unit  $W_w$ . The radius of influence ( $\delta$ ) is determined by the distribution of the

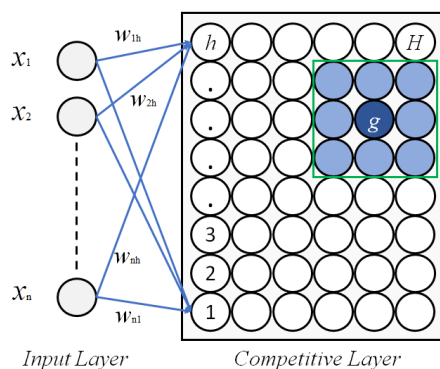


Fig. 3 SOM structure

neural units  $W_w$ ,  $W_B$  and  $W_A$ , which correspond to potential regions in the input. Therefore,  $\delta$  is calculated as the median distance obtained from the distances between the optimal solution  $g$  and the three units:  $W_w$ ,  $W_B$  and  $W_A$ .

$$\delta = \frac{D_B + D_W + D_A}{3} \quad (16)$$

The value of  $\delta$  is then used to create a 2-dimensional function, which is shown in Fig. 4. Once this value has been determined, a model is employed to generate  $N$  new solutions, using Eq. (17):

$$P_j(k+1) = \delta \times R \times r + W_w, \quad (17)$$

where  $r$  is a uniform random number ranging between -1 to 1.

### 3.5 Construct a new set of training

After creating the  $N$  new solutions, the next step is to generate the new learning set  $T(k+1)$  for the next iteration. As each iteration generates  $N$  new solutions, after several iterations, a significant amount of historical data is accumulated in  $H(k)$ . The learning set is composed of  $2N$  solutions. The initial  $N$  solutions in  $T(k+1)$  are the newly created ones, while the other  $N$  solutions are randomly selected from the historical data in  $H(k)$ . Once  $T(k+1)$  is

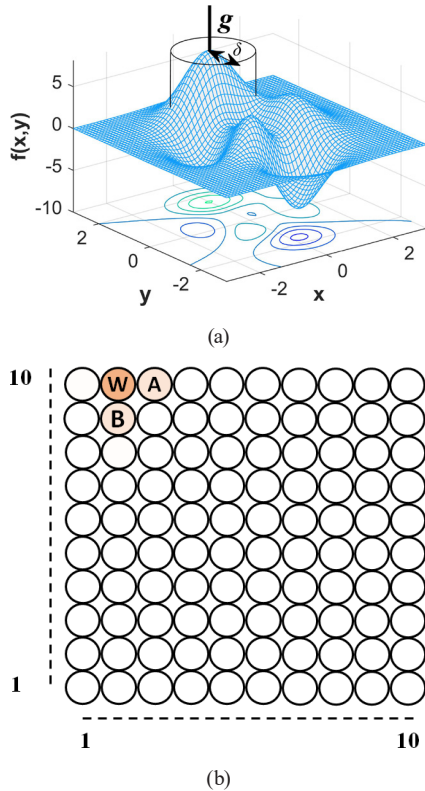


Fig. 4  $\delta$  representation for a 2D function; (a) objective function; (b) the competitive layer

created, the recently generated solutions  $P(k+1)$  are stored in a memory history, and  $H(k+1)$  is updated to be the union of  $P(k+1)$  and  $H(k)$ .

### 3.6 Calculation process

To use EASOM, the user inputs two parameters:  $N$ , the number of possible solutions to generate, and  $Maxgen$ , the maximum number of generations. The algorithm starts by creating an initial population  $P(0)$  of  $2N$  possible solutions. The SOM learns from the components in  $T(k)$  and selects the fittest item, which is denoted as  $g$ . The algorithm identifies the three neuronal units with the highest similarity to  $g$ , and feedback from them is used to calculate  $R$  and  $\delta$ .

Next,  $N$  new solutions are generated near  $W_w$  using the value of  $\delta$ . The new learning set  $T(k+1)$  is formed by combining the  $N$  new solutions with items from the historical data in  $H(k)$ . Specifically, the first  $N$  items in  $T(k+1)$  are the newly generated solutions, while the other  $N$  items are randomly selected from  $H(k)$ . The newly generated items are stored in  $P(k+1)$ , and  $H(k+1)$  is updated to include them.

The process is repeated until  $Maxgen$  is reached, with each iteration generating a new set of  $N$  solutions and updating the learning set and historical data. Fig. 5 illustrates the entire procedure for EASOM.

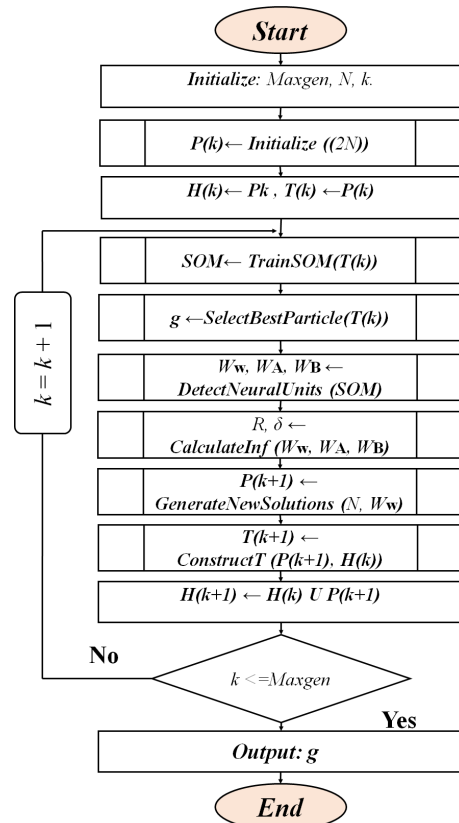


Fig. 5 EASOM algorithm

Fig. 6 presents the algorithm proposed for extracting the solar model parameter. The algorithm starts by initializing the solar PV model and reading the current and voltage measurements. Then, the EASOM algorithm is used to locate the strongest candidate (denoted as  $g$ ), with the aim of minimizing Eq. (11), which represents the cost function. Finally, EASOM outputs the best solution for either SDM or DDM.

### 4 Results and discussion

The proposed EASOM algorithm (Fig. 6) was employed to estimate parameters for solar PV models using the STM6-40/36 PV modules [23] (for SDM and DDM model) and compared to the algorithm SFO (sunflower optimization algorithm) [24], WOS (war strategy optimization algorithm) [25], modified JAYA [26], and GBO (Gradient-Based Optimizer) [27]. The STM6-40/36 module is monocrystalline and has 36 cells in series. To obtain the PV model parameters, the EASOM algorithm parameters is set in Table 2.

#### 4.1 Single diode

The objective is to extract the five parameters:  $I_{sd}$ ,  $I_{ph}$ ,  $R_s$ ,  $R_{sh}$  and  $n$  of an SDM for a PV solar cell. Table 3 displays the upper and lower limits of these parameters. The I-V and P-V characteristics of the PV using EASOM, SFO, WOS, modified JAYA, and GBO are illustrated in Figs. 7 and 8. The convergence curves for the loss functions are depicted in Fig. 9, and the absolute current error is plotted in Fig. 10. The extracted parameters by EASOM are listed in Table 4.

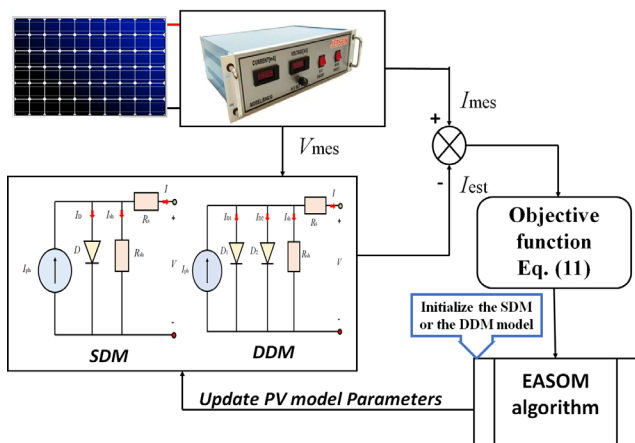


Fig. 6 The proposed EASOM

Table 2 EASOM parameter

Model	Population number ( $N$ )	Number of iterations $Maxgen$	Number of decision variables
SDM	1000	50	1
DDM	1000	50	1

Table 3 Limits of the SDM model

Parameter	Upper bound ( $ui$ )	Lower bound ( $li$ )
$I_{sd}$	50	0
$I_{ph}$	2	0
$R_s$	2	0
$R_{sh}$	2000	0
$n$	50	1

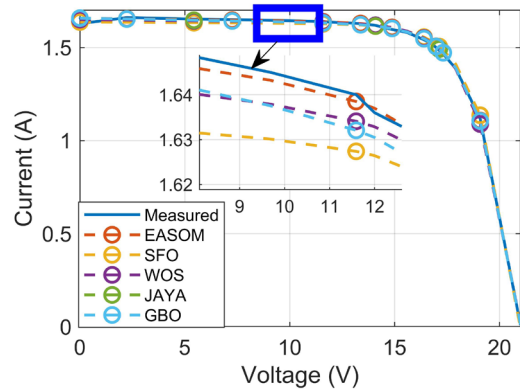


Fig. 7 I-V curve: estimated and measured of SDM model (STM6)

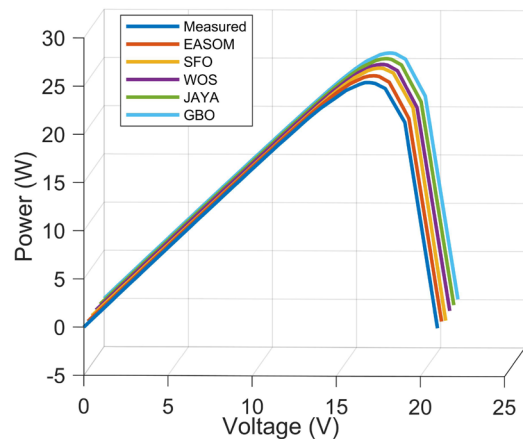


Fig. 8 Power curve P-V of the SDM model (STM6)

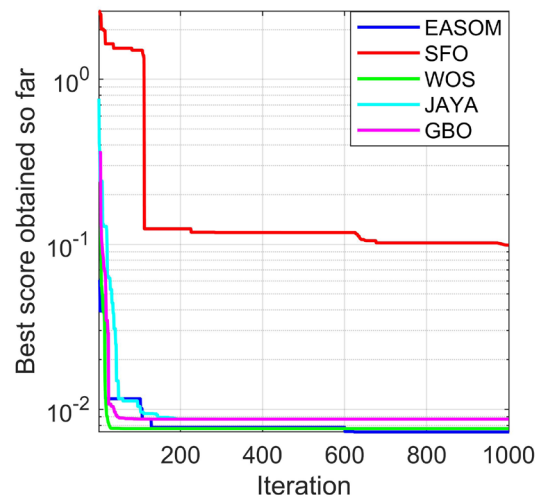


Fig. 9 Convergence curve SDM (STM6)

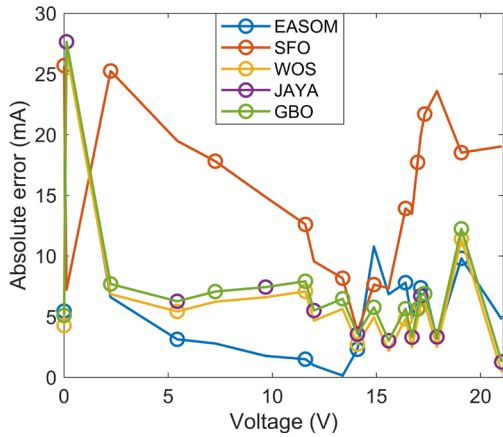


Fig. 10 Absolute current error in SDM model (STM6)

Table 4 Parameter extracted by EASOM for the SDM model

Method	$I_{ph}$	$I_{sd}$	$R_s$	$R_{sh}$	$n$
EASOM	1.6592	0.19382	0.3879	487.201	50

Table 5 Limits of the DDM model

Parameter	Upper bound ( $ui$ )	Lower bound ( $li$ )
$I_{sd1}$	2	0
$I_{sd2}$	50	0
$I_{ph}$	2	0
$R_s$	2	0
$R_{sh}$	2000	0
$n_1$	70	1
$n_2$	60	1

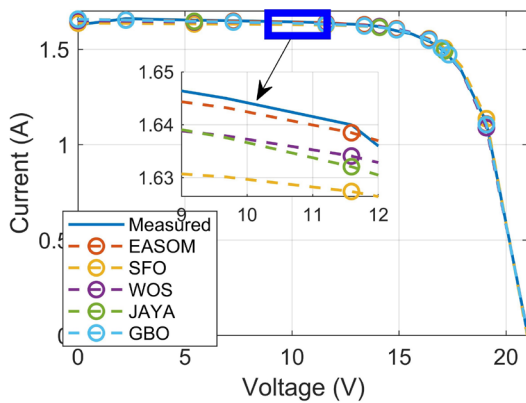


Fig. 11 I-V curve: estimated and measured of DDM model (STM6)

#### 4.2 Double diode

For the DDM case, seven parameters, namely  $I_{sd1}$ ,  $I_{ph}$ ,  $I_{sd2}$ ,  $R_s$ ,  $R_{sh}$ ,  $n_1$ ,  $n_2$  need to be extracted. The lower and upper bounds for these parameters are provided in Table 5.

Figs. 11 and 12 display the I-V and P-V characteristics of the PV employing EASOM, SFO, WOS, modified JAYA, and GBO. The convergence curves for the loss functions are illustrated in Fig. 13, while Fig. 14 shows the plot for the absolute current error. The extracted parameters by EASOM are listed in Table 6.

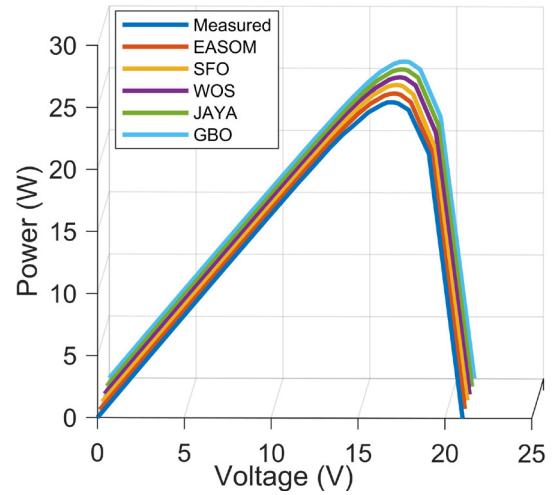


Fig. 12 Power curve P-V of the DDM model (STM6)

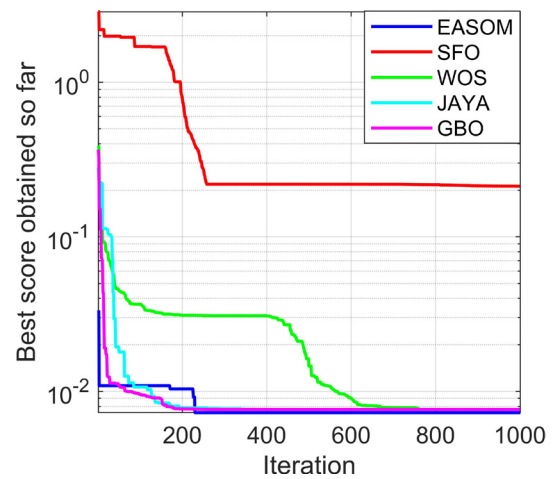


Fig. 13 Convergence curve DDM (STM6)

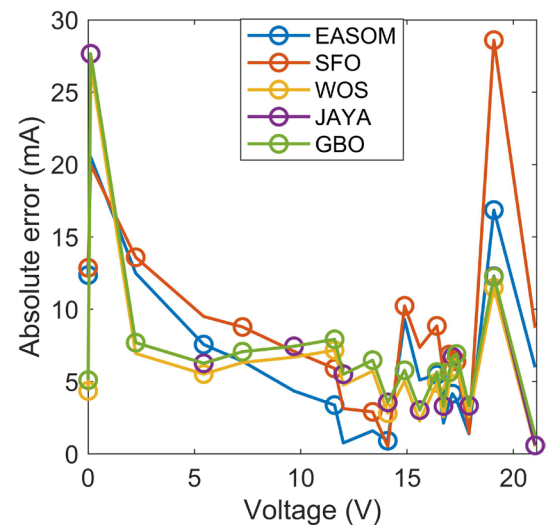


Fig. 14 Absolute current error in DDM model (STM6)

Table 6 Parameter extracted by EASOM for the DDM model

Method	$I_{sd1}$	$I_{sd2}$	$I_{ph}$	$R_s$	$R_{sh}$	$n_1$	$n_2$
EASOM	0.5634	0.37	1.6511	0.3506	1053.59	64.58	51.85

### 4.3 Discussion

In order to evaluate the effectiveness of the algorithms, we gauge their predictive performance through three variables: mean squared error (MSE) (Eq. (18)), normalized root mean squared error (NRMSE) (Eq. (19)), and root mean square error (RMSE) (Eq. (20)) expressed as:

$$MSE = \frac{1}{p} \sum_{i=1}^p (I_{est}(i) - I_{true}(i))^2, \quad (18)$$

$$NRMSE = \frac{RMSE}{I_{est,max} - I_{est,min}}, \quad (19)$$

$$RMSE = \sqrt{\frac{1}{p} \sum_{i=1}^p (I_{est}(i) - I_{true}(i))^2}, \quad (20)$$

where  $p$  is the number of points,  $I_{true}$  is the measured output voltage, and  $I_{est}$  is the estimated value.

Table 7 shows the predictive performance indicators of the algorithms used to estimate the PV solar parameters for the STM6-40/36 case. The RMSE, NRMSE, and mean MSE are used to evaluate the performance of the algorithms.

Looking at the results for the SDM case, the EASOM, JAYA, WOS, and GBO algorithms perform similarly well, with RMSE values of 8.3 and 8.7 mA, respectively. However, the NRMSE value of the compared algorithms (5.2) is higher than that of EASOM (4.99), indicating that EASOM performs slightly better in terms of accuracy. The SFO algorithm shows significantly worse performance with an RMSE value of 16.6 mA and a high NRMSE value of 10.

For the DDM case, the EASOM algorithm has the lowest RMSE value of 8.3 mA, followed by WOS, JAYA, and GBO with an RMSE value of 8.7 mA. The SFO algorithm has an RMSE value of 8.7 mA, which is similar to that of WOS but has a higher NRMSE value of 6.5.

**Table 7** Predictive performance indicators for STM for SDM and DDM

Model	Methods	RMSE (mA)	NRMSE	MSE
STM6 SDM	EASOM	8.30	4.99	6.89e-05
	WOS	8.70	5.20	7.57e-05
	SFO	16.6	10	2.76e-04
	JAYA	8.7	5.23	7.5768e-05
	GBO	8.704	5.21	7.5768e-05
STM6 DDM	EASOM	8.30	5	6.87e-05
	WOS	8.70	5.20	7.57e-05
	SFO	8.70	6.50	1.16e-04
	JAYA	8.705	5.22	7.5758e-05
	GBO	8.704	5.2	7.5768e-05

The MSE value is a measure of the quality of a predictive model and reflects how close the predicted values are to the actual values.

Looking at the MSE values, we can see that: EASOM has the lowest MSE values for both SDM and DDM cases, which suggests that it is the most accurate method among the three. In SDM, the MSE value for EASOM is 6.89e-05, while in DDM, it is 6.87e-05. Therefore, EASOM is a reliable method for both SDM and DDM cases, and it can provide accurate predictions. WOS, JAYA, and GBO exhibit the second-lowest MSE values, approximately 7.57e-05, for both SDM and DDM scenarios.

SFO has the highest MSE values among the three methods for both SDM and DDM cases. In SDM, the MSE value for SFO is 2.76e-04, while in DDM, it is 1.16e-04.

Table 8 provides a summary of the performance of three different algorithms (EASOM, WOS, and SFO) used to estimate the PV solar parameters SDM and DDM. Table 8 reports the maximum, minimum, mean, and power errors (Eq. (21)) for each algorithm and model.

Comparing the performance of the algorithms, the EASOM algorithm appears to have the best performance overall, achieving the lowest maximum and minimum error for both profiles. The WOS, JAYA, and GBO algorithm's performance is relatively similar to that of the EASOM algorithm, with only slightly higher maximum and minimum error values. The SFO algorithm, on the other hand, performs significantly worse, with the highest maximum and power error values and relatively high mean error values.

When comparing the performance of the algorithms between in SDM and DDM, some differences are also observed. For example, the EASOM algorithm achieves a lower maximum error for the DDM profile than for the

**Table 8** Absolute maximum, minimum, mean, and power error for the algorithms used to estimate the PV solar parameters for STM6

Pro-files	Methods	Max. error (mA)	Min. error (mA)	Mean error (mA)	Power error (mW)
STM6 SDM	EASOM	27.370	0.152	6.060	66.040
	WOS	27.640	1.259	6.920	70.230
	SFO	25.680	3.762	15.360	186
	JAYA	27.654	1.260	6.930	70.230
	GBO	27.653	1.266	6.931	70.205
STM6 DDM	EASOM	20.520	0.760	6.400	62.805
	WOS	27.650	1.260	6.930	70.205
	SFO	28.590	0.520	8.780	99.10
	JAYA	27.652	0.590	6.890	69.560
	GBO	27.651	1.260	6.930	70.205

SDM, while the WOS algorithm achieves the same maximum error for both profiles. However, the SFO algorithm performs worse for both models, achieving a higher maximum error and power error.

$$P_{w_{error}} = \frac{1}{n} \sum_{i=1}^n |P_{est}(i) - P_{true}(i)| \quad (21)$$

In Eq. (21)  $P_{est}$  and  $P_{true}$  are respectively the estimated and true measured power.

Overall, Tables 7 and 8 provide a useful summary of the performance of different algorithms in estimating the PV solar parameters. The results suggest that the EASOM is a promising method to achieve PV solar parameter estimation.

### 5 Applications, recommendations and future scope

The present work offers several potential applications and recommendations for future research in the field of solar PV parameter identification. The proposed algorithm, EASOM, can be utilized to enhance the accuracy and efficiency of solar PV parameter estimation in a variety of contexts. Researchers can apply this algorithm to improve the performance of existing solar PV models or to develop new models that accurately represent the behavior of solar cells under different environmental conditions. In addition, the use of self-organizing maps can be extended to other meta-heuristic algorithms to enhance their performance in other optimization problems. Further research is needed to investigate the use of EASOM in combination with other optimization techniques to achieve even better results. Finally, the proposed algorithm can be adapted for use in other renewable energy systems, such as wind or hydroelectric power, to improve their efficiency and performance. Overall, the present work represents an important contribution to the field of solar PV parameter estimation and offers valuable insights for researchers seeking to improve the accuracy and efficiency of renewable energy systems.

### 6 Conclusion

To summarize, we introduced a novel algorithm called enhanced self-organization maps (EASOM) for parameter estimation in solar PV models. By leveraging self-organization maps, EASOM is able to effectively reduce the search space for parameter estimation.

We verified the performance of EASOM by extracting parameters from the single diode (SDM) and double diode (DDM) models for the STM6-40/36 PV module. In comparison to state-of-the-art algorithms such as WOS and

SFO, JAYA and GBO. EASOM consistently outperformed these methods for both SDM and DDM models.

EASOM outperformed the other algorithms, achieving the lowest RMSE and MSE values of 8.3 mA and 6.87e-05, respectively, for both SDM and DDM models. Additionally, EASOM exhibited the lowest maximum error values of 27.37 mA and 20.52 mA for SDM and DDM, respectively, as well as low power error of 66.04 mW and 62.8 mW, further highlighting its superior performance.

These results suggest that the EASOM algorithm has significant potential for accurately estimating the parameters of solar PV systems and represents a promising avenue for future research in this area.

### Nomenclature

$I$	Output current
$I_{sh}$	Shunt resistance current
$R_s$	Series resistance
$I_{ph}$	Photocurrent
$I_D, I_{D1}$ and $I_{D2}$	The current flowing through the diode
$I_{sd}, I_{sd1}$ and $I_{sd2}$	The reverse diode saturation
$R_{sh}$	The shunt resistance
$q$	The electron charge (1.602e-19 C)
$K$	The Boltzmann constant
$V$	The cell output voltage
$n, n_1$ and $n_2$	The diode ideality factor
$T$	The temperature in kelvin
$N_p$	Solar cells arranged in parallel
$N_s$	Solar cells arranged in series
$I_{estim}$	The estimated current
$I_{mes}$	The measured current
$Maxgen$	Maximum iteration limit
$li$	The lower boundary
$ui$	The upper boundary
$g$	The best solution discovered so far
$P(k)$	Potential solutions
$T(k)$	Data points
$W_w, W_A$ and $W_B$	Neuronal units
$w$	The selected neural unit
$D_w$	The distance between the unit $W_w$ and $g$
$D_B$	The distance between the unit $W_B$ and $g$
$D_A$	The distance between the unit $W_A$ and $g$
$R$	The positional rank
$\delta$	The radius of influence
$r$	A uniform random number [-1, 1]
$N$	Population number
MSE	Mean squared error

NRMSE	Normalized root mean squared error	$P_{est}$	The estimated power
RMSE	Root mean square error	$P_{true}$	The true measured power
$P_{error}$	The power error	$H(k)$	Historical data

## References

- [1] Soonmin, H., Taghavi, M. "Solar energy development: Study cases in Iran and Malaysia", *International Journal of Engineering Trends and Technology*, 70(8), pp. 408–422, 2022.  
<https://doi.org/10.14445/22315381/IJETT-V70I8P242>
- [2] Alhousni, F. K., Ismail, F. B., Okonkwo, P. C., Mohamed, H., Okonkwo, B. O., Al-Shahri, O. A. "A review of PV solar energy system operations and applications in Dhofar Oman", *AIMS Energy*, 10(4), pp. 858–884, 2022.  
<https://doi.org/10.3934/energy.2022039>
- [3] Selem, S. I., Hasanien, H. M., El-Fergany, A. A. "Parameters extraction of PEMFC's model using manta rays foraging optimizer", *International Journal of Energy Research*, 44(6), pp. 4629–4640, 2020.  
<https://doi.org/10.1002/er.5244>
- [4] Wang, M., Zhao, X., Heidari, A. A., Chen, H. "Evaluation of constraint in photovoltaic models by exploiting an enhanced ant lion optimizer", *Solar Energy*, 211, pp. 503–521, 2020.  
<https://doi.org/10.1016/j.solener.2020.09.080>
- [5] Chen, X., Tianfield, H., Mei, C., Du, W., Liu, G. "Biogeography-based learning particle swarm optimization", *Soft Computing*, 21(24), pp. 7519–7541, 2017.  
<https://doi.org/10.1007/s00500-016-2307-7>
- [6] Xiong, G., Zhang, J., Shi, D., Zhu, L., Yuan, X., Tan, Z. "Winner-leading competitive swarm optimizer with dynamic Gaussian mutation for parameter extraction of solar photovoltaic models", *Energy Conversion and Management*, 206, 112450, 2020.  
<https://doi.org/10.1016/j.enconman.2019.112450>
- [7] Batzelis, E. I., Papanthanasios, S. A. "A method for the analytical extraction of the single-diode PV model parameters", *IEEE Transactions on Sustainable Energy*, 7(2), pp. 504–512, 2016.  
<https://doi.org/10.1109/TSTE.2015.2503435>
- [8] Changmai, P., Nayak, S. K., Metya, S. K. "Estimation of PV module parameters from the manufacturer's datasheet for MPP estimation", *IET Renewable Power Generation*, 14(11), pp. 1988–1996, 2020.  
<https://doi.org/10.1049/iet-rpg.2019.1377>
- [9] Huang, Y.-C., Huang, C.-M., Chen, S.-J., Yang, S.-P. "Optimization of module parameters for PV power estimation using a hybrid algorithm", *IEEE Transactions on Sustainable Energy*, 11(4), pp. 2210–2219, 2020.  
<https://doi.org/10.1109/TSTE.2019.2952444>
- [10] Saadaoui, D., Elyaqouti, M., Assalaou, K., Ben hmamou, D., Lidaighbi, S. "Parameters optimization of solar PV cell/module using genetic algorithm based on non-uniform mutation", *Energy Conversion and Management: X*, 12, 100129, 2021.  
<https://doi.org/10.1016/j.ecmx.2021.100129>
- [11] Gao, S., Wang, K., Tao, S., Jin, T., Dai, H., Cheng, J. "A state-of-the-art differential evolution algorithm for parameter estimation of solar photovoltaic models", *Energy Conversion and Management*, 230, 113784, 2021.  
<https://doi.org/10.1016/j.enconman.2020.113784>
- [12] Muhsen, D. H., Ghazali, A. B., Khatib, T., Abed, I. A. "Parameters extraction of double diode photovoltaic module's model based on hybrid evolutionary algorithm", *Energy Conversion and Management*, 105, pp. 552–561, 2015.  
<https://doi.org/10.1016/j.enconman.2015.08.023>
- [13] Touabi, C., Ouadi, A., Bentarzi, H. "Photovoltaic Panel Parameters Estimation Using an Opposition Based Initialization Particle Swarm Optimization", *Engineering Proceedings*, 29(1), 16, 2023.  
<https://doi.org/10.3390/engproc2023029016>
- [14] Pan, M., Li, C., Gao, R., Huang, Y., You, H., Gu, T., Qin, F. "Photovoltaic power forecasting based on a support vector machine with improved ant colony optimization", *Journal of Cleaner Production*, 277, 123948, 2020.  
<https://doi.org/10.1016/j.jclepro.2020.123948>
- [15] Jordehi, A. R. "Gravitational search algorithm with linearly decreasing gravitational constant for parameter estimation of photovoltaic cells", In: 2017 IEEE Congress on Evolutionary Computation (CEC), Donostia, Spain, 2017, pp. 37–42. ISBN 978-1-5090-4602-7  
<https://doi.org/10.1109/CEC.2017.7969293>
- [16] Li, S., Gong, W., Yan, X., Hu, C., Bai, D., Wang, L., Gao, L. "Parameter extraction of photovoltaic models using an improved teaching-learning-based optimization", *Energy Conversion and Management*, 186, pp. 293–305, 2019.  
<https://doi.org/10.1016/j.enconman.2019.02.048>
- [17] Premkumar, M., Sowmya, R., Jangir, P., Siva Kumar, J. S. V. "A new and reliable objective functions for extracting the unknown parameters of solar photovoltaic cell using political optimizer algorithm", In: 2020 International Conference on Data Analytics for Business and Industry: Way Towards a Sustainable Economy (ICDABI), Sakheer, Bahrain, 2020, pp. 1–6. ISBN 978-1-7281-9676-3  
<https://doi.org/10.1109/ICDABI51230.2020.9325627>
- [18] Ben Messaoud, R. "Extraction of uncertain parameters of double-diode model of a photovoltaic panel using Ant Lion Optimization", *SN Applied Sciences*, 2(2), 239, 2020.  
<https://doi.org/10.1007/s42452-020-2013-z>
- [19] Cárdenas, A. A., Carrasco, M., Mancilla-David, F., Street, A., Cárdenas, R. "Experimental parameter extraction in the single-diode photovoltaic model via a reduced-space search", *IEEE Transactions on Industrial Electronics*, 64(2), pp. 1468–1476, 2017.  
<https://doi.org/10.1109/TIE.2016.2615590>
- [20] Abbassi, A., Gammoudi, R., Dami, M. A., Hasnaoui, O., Jemli, M. "An improved single-diode model parameters extraction at different operating conditions with a view to modeling a photovoltaic generator: A comparative study", *Solar Energy*, 155, pp. 478–489, 2017.  
<https://doi.org/10.1016/j.solener.2017.06.057>

- [21] Abdel-Basset, M., Mohamed, R., Chakraborty, R. K., Sallam, K., Ryan, M. J. "An efficient teaching-learning-based optimization algorithm for parameters identification of photovoltaic models: Analysis and validations", *Energy Conversion and Management*, 227, 113614, 2021.  
<https://doi.org/10.1016/j.enconman.2020.113614>
- [22] Cuevas, E., Galvez, J. "An optimization algorithm guided by a machine learning approach", *International Journal of Machine Learning and Cybernetics*, 10(11), pp. 2963–2991, 2019.  
<https://doi.org/10.1007/s13042-018-00915-0>
- [23] Li, S., Gong, W., Yan, X., Hu, C., Bai, D., Wang, L. "Parameter estimation of photovoltaic models with memetic adaptive differential evolution", *Solar Energy*, 190, pp. 465–474, 2019.  
<https://doi.org/10.1016/j.solener.2019.08.022>
- [24] Qais, M. H., Hasanien, H. M., Alghuwainem, S. "Identification of electrical parameters for three-diode photovoltaic model using analytical and sunflower optimization algorithm", *Applied Energy*, 250, pp. 109–117, 2019.  
<https://doi.org/10.1016/j.apenergy.2019.05.013>
- [25] Ayyarao, T. S. L. V., Kumar, P. P. "Parameter estimation of solar PV models with a new proposed war strategy optimization algorithm", *International Journal of Energy Research*, 46(6), pp. 7215–7238, 2022.  
<https://doi.org/10.1002/er.7629>
- [26] Luu, T. V., Nguyen, N. S. "Parameters extraction of solar cells using modified JAYA algorithm", *Optik*, 203, 164034, 2020.  
<https://doi.org/10.1016/j.ijleo.2019.164034>
- [27] Ismaeel, A. A. K., Houssein, E. H., Oliva, D., Said, M. "Gradient-based optimizer for parameter extraction in photovoltaic models", *IEEE Access*, 9, pp. 13403–13416, 2021.  
<https://doi.org/10.1109/ACCESS.2021.3052153>